Title

Optimal dispatch of reactive power for voltage regulation and balancing in unbalanced distribution systems

Authors

Arnold, Daniel B
Sankur, Michael
Dobbe, Roel
et al.

Publication Date

2016-07-17

Peer reviewed

Optimal Dispatch of Reactive Power for Voltage Regulation and Balancing in Unbalanced Distribution Systems

Daniel B. Arnold*, Michael Sankur*, Roel Dobbe**, Kyle Brady**,
Duncan S. Callaway***, and Alexandra Von Meier**
*Department of Mechanical Engineering
**Department of Electrical Engineering and Computer Science
***Energy and Resources Group
University of California, Berkeley
Berkeley, California 94720
(dbarnold, msankur, dobbe, kwbrady, dcal, vonmeier) @berkeley.edu

***Abstract*—Optimization of distributed power assets is a powerful tool that has the potential to assist utility efforts to ensure customer voltages are within pre-defined tolerances and to improve distribution system operations. While convex relaxations of Optimal Power Flow (OPF) problems have been proposed for both balanced and unbalanced networks, these approaches do not provide universal convexity guarantees and scale inefficiently as network size and the number of constraints increase. In balanced networks, a linearized model of power flow, the LinDistFlow model, has been successfully employed to solve approximate OPF problems quickly and with high degrees of accuracy. In this work, an extension of the LinDistFlow model is proposed for unbalanced distribution systems, and is subsequently used to formulate an approximate unbalanced OPF problem that uses VAR assets for voltage balancing and regulation. Simulation results on the IEEE 13 node test feeder demonstrate the ability of the unbalanced LinDistFlow model to perform voltage regulation and balance system voltages.**

NOMENCLATURE

$V_{\phi,k}$: Voltage phasor at node k on phase ϕ
$\mathbb{V}_k$: Vector of voltage phasors at node k
$y_{\phi,k}$: Square magnitude of voltage at node k on phase ϕ
$\mathbb{Y}_k$: Vector of square magnitudes of voltage at node k
$Z_{\phi\phi,jk}$: Impedance of segment (j,k) on phase ϕ
$Z_{\phi\psi,jk}$: Impedance of segment (j,k) between phases (ϕ,ψ)
$\mathbb{Z}_{jk}$: Impedance matrix of line segment (j,k)
$I_{\phi,k}$: Current phasor entering node k on phase ϕ
$\mathbb{I}_k$: Vector of current phasors entering node k
$i_{\phi,k}$: Load current of phase ϕ at node k
$\mathbf{i}_k$: Vector of load currents at node k
$S_{\phi,k}$: Phasor of complex power entering node k on phase ϕ
$\mathbb{S}_k$: Vector of complex power phasors entering node k
$s_{\phi,k}$: Complex load on phase ϕ at node k
$\mathbf{s}_k$: Vector of complex loads at node k
$u_{\phi,k}$: Inverter VAR dispatch on phase ϕ at node k

This work was supported in part by the U.S. Department of Energy ARPA-E program (DE-AR0000340).

I. INTRODUCTION

Coordination of a diverse set of Distributed Energy Resources (DER) presents many challenges to utility operators, who strive to ensure power of sufficient quality and quantity is available to retail customers at least cost. Such assets can vary in size from residential rooftop PV units to larger PV arrays and, perhaps, battery storage systems located at residential, commercials and industrial sites. As has been experienced in Hawaii [1], the negative impact of high levels of distributed PV under current interconnection standards is significant, and has led to financial impacts to both consumers and the utility. However, distributed generation resources could, under the correct operational control scenarios, provide numerous benefits to the grid, including voltage support and VAR compensation.

A variety of strategies for the management of DER presently exist for *balanced* distribution system models. Turitsyn et al. [2] considered a suite of distributed control strategies for reactive power compensation using four quadrant inverters. The work of [3] studies distributed voltage regulation in the absence of communication, relying on locally obtained information. Their results extend to optimize the cost of reactive power and are based on linearized power flow approximations. In [4], a two-stage control architecture for voltage regulation is considered where distributed controllers inject power based on local sensitivity measurements. The authors of [5] study local voltage reference tracking with integral-type controllers, based on local voltage measurements. The authors of [6] address voltage regulation and loss minimization through solving an Optimal Power Flow (OPF) problem, and address convexity issues using second order cone relaxations. The work of [7] also considers an OPF approach for voltage regulation in distribution networks by framing the decision-making process a semidefinite program. The authors provide conditions under which the semidefinite relaxation of the nonconvex power flow problem is tight in balanced circuits. It is worth noting that many of the aforementioned approaches can be traced back to

978-1-5090-4168-8/16/$31.00 ©2016 IEEE

the seminal work of [8], that introduced nonlinear and linear-approximated recursive branch power flow models.

Approaches to coordinate DER in *unbalanced* distribution systems are much less prevalent. Perhaps the best known efforts have been put forth by the authors of [9], who consider semidefinite relaxations for OPF problems in unbalanced systems, but do not provide conditions under which optimality is guaranteed. In addition to inefficient scaling as the problem size increases, the work of [10] points out that it becomes more difficult to find a tight relaxation as the ratio of constraints to network buses increases. A likely reason that more strategies focusing on coordination of distributed energy resources in unbalanced systems do not exist is the lack of suitable linear models that approximate three phase power flow.

This work attempts to fill that void by proposing a linearized unbalanced power flow model that can be viewed as an extension of the *LinDistFlow* [8] linear approximation for balanced systems. Using this linear model, we construct an OPF formulation that dispatches reactive power resources from controllable power electronic inverters to perform voltage balancing and regulation. Our results show that OPF formulations that utilize the linearized three phase *LinDistFlow* model results in a dispatch of inverter VAR resources that successfully drives system voltages into acceptable regimes and simultaneously balances voltages by reducing magnitude differences between phases.

This work is organized as follows. A model of nonlinear three phase unbalanced power flow is introduced in Section II. This model, used in simulations later in the paper, is also used in the derivation of the linear approximation for three phase power flow in Section III. In Section IV, we formulate an OPF to perform voltage regulation and balancing, and discuss results from simulation. Finally, concluding remarks are provided in Section V.

II. Preliminaries

Let $T = (H, E)$ denote rooted tree graph representing a balanced radial distribution feeder, where H is the set of nodes of the feeder and the transmission link and E is the set of line segments. Nodes are indexed by $i = 0, 1, \ldots, m$, where m is the order (number of nodes) of the distribution feeder, and node 0 denotes the feeder head (or substation). We treat node 0 as an infinite bus, decoupling interactions in the downstream distribution system from the rest of the grid. While the substation voltage may evolve over time, we assume this evolution takes place independently of our inverter control action. For adjacent nodes j and k, the current/voltage relationship is captured by KVL and KCL:

$$\begin{bmatrix} V_a \\ V_b \\ V_c \end{bmatrix}_j = \begin{bmatrix} V_a \\ V_b \\ V_c \end{bmatrix}_k + \begin{bmatrix} Z_{aa} & Z_{ab} & Z_{ac} \\ Z_{ba} & Z_{bb} & Z_{bc} \\ Z_{ca} & Z_{cb} & Z_{cc} \end{bmatrix}_{jk} \begin{bmatrix} I_a \\ I_b \\ I_c \end{bmatrix}_k \tag{1}$$

$$\begin{bmatrix} I_a \\ I_b \\ I_c \end{bmatrix}_j = \begin{bmatrix} i_a \\ i_b \\ i_c \end{bmatrix}_j + \sum_{k:(j,k)\in E} \begin{bmatrix} I_a \\ I_b \\ I_c \end{bmatrix}_k, \tag{2}$$

where i_a denotes phase a load current, and Z_{aa} and Z_{ab} are the self impedance for phase a and mutual impedance between phases a and b, etc.. We assume that each node serves a complex load in each phase, $s_{\phi,k} = V_{\phi,k} i^*_{\phi,k}$ whose real and reactive power components are given by (3) and (4), respectively.

$$p_{\phi,k}(V_{\phi,k}) = p_{\phi,k}\left(a^0_{\phi,k} + a^1_{\phi,k}\left|V_{\phi,k}\right|^2\right) \tag{3}$$

$$q_{\phi,k}(V_{\phi,k}) = q_{\phi,k}\left(a^0_{\phi,k} + a^1_{\phi,k}\left|V_{\phi,k}\right|^2\right) + u_{\phi,k} \tag{4}$$

where $a^0_k + a^1_k = 1$ and are, for simplicity, assumed constant across all phases at each node. $u_{\phi,k}$ is the reactive power that can be sourced or consumed from a VAR resource on phase ϕ at node k. In our convention, positive demand denotes power consumption and negative demand is power injected, or supplied, to the grid. Equations (1)–(4) represent the power flow model that will be used to generate simulations in Section IV.

III. Derivation of Linearized Model

In this section, we derive a linear approximation of three phase power flow. This model can be thought of as an extension of the *LinDistFlow* model to unbalanced circuits. Consider two adjacent nodes of the distribution feeder, $(j, k) \in H$. We begin by expressing (1)–(2) in vector form:

$$\mathbb{V}_j = \mathbb{V}_k + \mathbb{Z}_k \mathbb{I}_k \tag{5}$$

$$\mathbb{I}_j = \mathbf{i}_j + \sum_{k:(j,k)\in E} \mathbb{I}_k. \tag{6}$$

We now right multiply each side of (5) by its complex conjugate and right multiply both sides of (6) by $\mathbb{V}^*_j$ and take the complex conjugate, resulting in:

$$\begin{aligned} \mathbb{V}_j \mathbb{V}^*_j &= \mathbb{V}_k \mathbb{V}^*_k + \mathbb{Z}_k \mathbb{I}_k \mathbb{V}^*_k + \mathbb{V}_k \mathbb{I}^*_k \mathbb{Z}^*_k + \mathbb{Z}_k \mathbb{I}_k \mathbb{I}^*_k \mathbb{Z}^*_k \\ &= \mathbb{V}_k \mathbb{V}^*_k + 2\,\mathbf{Re}\left\{\mathbb{V}_k \mathbb{I}^*_k \mathbb{Z}^*_k\right\} + \mathbb{Z}_k \mathbb{I}_k \mathbb{I}^*_k \mathbb{Z}^*_k, \end{aligned} \tag{7}$$

$$\mathbb{V}_j \mathbb{I}^*_j = \mathbb{V}_j \mathbf{i}^*_j + \sum_{k:(j,k)\in E} \left(\mathbb{V}_k + \mathbb{Z}_k \mathbb{I}_k\right) \mathbb{I}^*_k. \tag{8}$$

Similar to the derivation of the *LinDistFlow* system, we neglect loss terms in (7)–(8), which yields:

$$\mathbb{V}_j \mathbb{V}^*_j \approx \mathbb{V}_k \mathbb{V}^*_k + 2\,\mathbf{Re}\left\{\mathbb{V}_k \mathbb{I}^*_k \mathbb{Z}^*_k\right\} \tag{9}$$

$$\mathbb{V}_j \mathbb{I}^*_j \approx \mathbb{V}_j \mathbf{i}^*_j + \sum_{k:(j,k)\in E} \mathbb{V}_k \mathbb{I}^*_k. \tag{10}$$

where (7)–(8) are 3×3 matrix equations. Focusing our attention first on (8), we apply the power equation $S_{\phi,k} = V_{\phi,k} I^*_{\phi,k}$ to the diagonal elements and collect these into the vector equation:

$$\mathbb{S}_j \approx \mathbf{s}_j + \sum_{k:(j,k)\in E} \mathbb{S}_k \tag{11}$$

Returning attention to (9), we expand $\mathbb{I}_k$ according to $S_{\phi,k} = V_{\phi,k} I^*_{\phi,k}$, resulting in:

$$\begin{aligned} &\mathbb{V}_j \mathbb{V}^*_j \approx \mathbb{V}_k \mathbb{V}^*_k + \\ &\quad 2\,\mathbf{Re}\left\{\mathbb{V}_k \begin{bmatrix} S_a V_a^{-1} & S_b V_b^{-1} & S_c V_c^{-1} \end{bmatrix}_k \mathbb{Z}^*_{jk}\right\} \end{aligned} \tag{12}$$

which is equivalent to:

978-1-5090-4168-8/16/$31.00 ©2016 IEEE

$$\mathbb{V}_j\mathbb{V}_j^* \approx \mathbb{V}_k\mathbb{V}_k^* + 2\,\mathbf{Re}\left\{\begin{bmatrix} S_a & V_aS_bV_b^{-1} & V_aS_cV_c^{-1} \\ V_bS_aV_a^{-1} & S_b & V_bS_cV_c^{-1} \\ V_cS_aV_a^{-1} & V_cS_bV_b^{-1} & S_c \end{bmatrix}_k \mathbb{Z}_{jk}^*\right\} \quad (13)$$

Note that even after neglecting the loss terms, (13) is still nonlinear. To further simplify the system, we adopt an approximation that assumes the ratio of voltage phasors are constant:

$$V_{a,k}V_{b,k}^{-1} \approx \alpha \quad V_{b,k}V_{c,k}^{-1} \approx \alpha \quad V_{a,k}V_{c,k}^{-1} \approx \alpha^2 \quad (14)$$

where

$$\alpha = 1\angle 120^\circ = \frac{-1+j\sqrt{3}}{2}, \quad \alpha^2 = 1\angle 240^\circ = -\frac{1+j\sqrt{3}}{2}. \quad (15)$$

The simplification of the quotient of the voltage phasors according to (14)–(15) transforms (13) into:

$$\mathbb{V}_j\mathbb{V}_j^* \approx \mathbb{V}_k\mathbb{V}_k^* + 2\,\mathbf{Re}\left\{\begin{bmatrix} S_a & \alpha S_b & \alpha^2 S_c \\ \alpha^2 S_a & S_b & \alpha S_c \\ \alpha S_a & \alpha^2 S_b & S_c \end{bmatrix}_k \mathbb{Z}_{jk}^*\right\} \quad (16)$$

Although (16) is a 3×3 matrix equation, we are intertested only in the diagonal elements, which we gather and place into 3×1 vectors resulting in (17):

$$\mathbb{Y}_j \approx \mathbb{Y}_k + 2\,\mathbf{Re}\left\{\begin{bmatrix} Z_{aa,jk}^*S_{a,k} + \alpha Z_{ab,jk}^*S_{b,k} + \alpha^2 Z_{ac,jk}^*S_{c,k} \\ \alpha^2 Z_{ba,jk}^*S_{a,k} + Z_{bb,jk}^*S_{b,k} + \alpha Z_{bc,jk}^*S_{c,k} \\ \alpha Z_{ca,jk}^*S_{a,k} + \alpha^2 Z_{cb,jk}^*S_{b,k} + Z_{cc,jk}^*S_{c,k} \end{bmatrix}\right\}, \quad (17)$$

where we have defined the vector of the square of voltage magnitudes in phases a, b, c as $\mathbb{Y}_k = \begin{bmatrix} y_a & y_b & y_c \end{bmatrix}_k^T$. The 3×1 vector inside the **Re** operator can be broken up into a 3×3 matrix of impedances for line segment (j,k) and a 3×1 vector of node k power injections, as is shown in (18).

$$\mathbb{Y}_j \approx \mathbb{Y}_k + 2\,\mathbf{Re}\left\{\begin{bmatrix} Z_{aa}^* & \alpha Z_{ab}^* & \alpha^2 Z_{ac}^* \\ \alpha^2 Z_{ba}^* & Z_{bb}^* & \alpha Z_{bc}^* \\ \alpha Z_{ca}^* & \alpha^2 Z_{cb}^* & Z_{cc}^* \end{bmatrix}_{jk} \begin{bmatrix} S_a \\ S_b \\ S_c \end{bmatrix}_k\right\} \quad (18)$$

Viewed in this form, the approximation to the ratio of voltage phasors essentially introduces $\pm 120^\circ$ rotations of the cross-phase impedances. Expanding the impedance matrix entries as $Z_{\phi\psi,k} = r_{\phi,\psi,k} + jx_{\phi,\psi,k}$, the complex power as $S_{\phi,k} = P_{\phi,k} + jQ_{\phi,k}$, and using the definition of α, it can be shown that (18) simplifies into the following linear matrix equation:

$$\mathbb{Y}_j \approx \mathbb{Y}_k - \mathbb{M}_{jk}^P\mathbb{P}_k - \mathbb{M}_{jk}^Q\mathbb{Q}_k \quad (19)$$

where

$$\mathbb{M}_{jk}^P = \begin{bmatrix} -2r_{aa} & r_{ab}-\sqrt{3}x_{ab} & r_{ac}+\sqrt{3}x_{ac} \\ r_{ba}+\sqrt{3}x_{ba} & -2r_{bb} & r_{bc}-\sqrt{3}x_{bc} \\ r_{ca}-\sqrt{3}x_{ca} & r_{cb}+\sqrt{3}x_{cb} & -2r_{cc} \end{bmatrix}_{jk} \quad (20)$$

$$\mathbb{M}_{jk}^Q = \begin{bmatrix} -2x_{aa} & x_{ab}+\sqrt{3}r_{ab} & x_{ac}-\sqrt{3}r_{ac} \\ x_{ba}-\sqrt{3}r_{ba} & -2x_{bb} & x_{bc}+\sqrt{3}r_{bc} \\ x_{ca}+\sqrt{3}r_{ca} & x_{cb}-\sqrt{3}r_{cb} & -2x_{cc} \end{bmatrix}_{jk}. \quad (21)$$

We now restate (11) for completeness:

$$\mathbb{S}_j \approx \mathbf{s}_j + \sum_{k:(j,k)\in E} \mathbb{S}_k \quad (22)$$

Equations (19)–(22) represent a linearized model of unbalanced distribution power flow that maps node k real and reactive power injections into squared voltage magnitude differences. As the system shows, power contribution in all three phases collectively influence each phase's squared voltage magnitude difference. It is easily verified that a reduction to a single phase network results in the *LinDistFlow* model discussed in [8].

IV. Simulation Results

In this section, we incorporate the linearized three phase power flow model into an OPF program. The goal of the optimization is to control inverter VAR resources in a distribution system to regulate and balance system voltages. We define the problem as:

$$\begin{aligned} \underset{u,y_i,Q_i,P_i}{\text{minimize}} \quad & \sum_{i\in H}\left[\sum_{\substack{\phi,\psi\in\{a,b,c\}\\ \phi\neq\psi}} (y_{\phi,i}-y_{\psi,i})^2\right] + \rho u_{\phi,i}^2 \\ \text{subject to} \quad & (19)-(22), \\ & \underline{y} \le y_i \le \overline{y}, \quad \forall i \in H, \end{aligned} \quad (23)$$

where ρ is positive (0.5 in simulations) and $\underline{y}$ and $\overline{y}$ represent upper and lower bounds on voltage magnitude (which are fixed to 0.95^2 and 1.05^2), respectively. The first term in the objective function is the sum squared Euclidean distances of squared voltage magnitude differences across phases at each node. The second term penalizes the use of inverter VAR resources.

The OPF is performed on the IEEE 13 test node distribution feeder [11], seen in Fig. 1. This simulation neglects the presence of the voltage regulator between nodes 650 and 632, the transformer between nodes 633 and 634, the switch (assumed closed) between nodes 671 and 692, and capacitors at nodes 675 and 611. Constant power and constant impedance load fractions were assigned as $a_i^0 = 0.85$ and $a_i^1 = 0.15$.

Feeder configurations, per-length line segment impedances, and line segment lengths can be found in [11]. All line segment impedances were increased by a factor of 1.25. Spot loads (also found in [11]) were assigned to nodes according to Table I. Distributed loads were neglected. For the simulation, feeder power and voltage base values were chosen as the power rating and secondary voltage of the substation transformer, 500kVA and 4.16kV respectively. Additionally, feeder head voltage was

978-1-5090-4168-8/16/$31.00 ©2016 IEEE

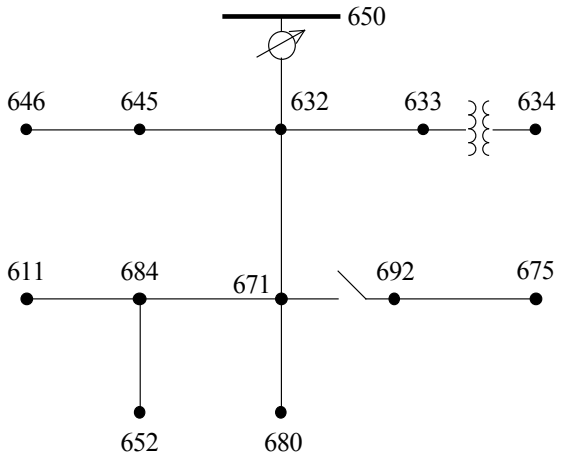

Fig. 1: IEEE 13 node feeder model.

fixed to 1 p.u.. Controllable three phase inverter resources were placed at nodes 632, 675, 680, and 684. These resources were purposefully left unconstrained to test the effectiveness of the OPF, with the ability to source or sink arbitrary amounts of reactive power.

TABLE I: SPOT LOADS OF 13 NODE FEEDER.

	Phase		
Node	a [pu]	b [pu]	c [pu]
650	0	0	0
632	0	0	0
633	0	0	0
634	0.032 + j 0.022	0.024 + j 0.018	0.024 + j 0.018
645	–	0.034 + j 0.025	0
646	–	0.046 + j 0.0264	0
671	0.077 + j 0.044	0.077 + j 0.044	0.077 + j 0.044
692	0	0	0.034 + j 0.0302
675	0.097 + j 0.038	0.0136 + j 0.012	0.058 + j 0.0424
680	0	0	0
684	0	–	0
652	0.0256 + j 0.0172	–	–
611	–	–	0.034 + j 0.0106
Total	0.2316 + j 0.1212	0.1946 + j 0.1254	0.227 + j 0.1506

Simulation results are presented in Figs. 2 - 5 and in Table II. Voltage profiles for the base scenario (where inverter VAR resources are not utilized) and control scenario (inverter VAR resources are determined by the OPF of (23)) can be seen in Fig. 2, with phase a, b and c voltage magnitudes plotted in Fig. 2a, Fig. 2b, and Fig. 2c, respectively. As the figures show, in the control case, the voltage magnitudes of phase a are kept almost constant with the base case. The voltage magnitudes of phase b are decreased, and of c are increased, to achieve greater voltage magnitude balance. Additionally, the voltages of phase c, originally in violation of the lower voltage bound, are now within the acceptable $\pm 5\%$ threshold. It should be noted that the rise in voltage magnitude for the base scenario from node 632 to node 671 reconciles with power-flow simulation results in [11] and is likely due to the fact that off diagonal components of (20)-(21) have *opposite* signs of the diagonal components, indicating that large voltage drops in some phases actually contribute to voltage *rises* in other phases.

A comparison of voltage magnitudes for all phases at each node can be seen in Fig. 3, with the base scenario in Fig. 3a, and the control scenario in Fig. 3b. As the figures show, the voltage magnitudes are much closer together when inverter reactive power is dispatched according to the results of the OPF of (23).

Figure 4 evaluates the first term of objective function of (23) for all nodes with and without control action. The results show that the objective function value (which measures the Euclidian distance between squared voltage magnitudes) decreases at all nodes following control action with the exception of node 646, which increases very slightly.

Optimal inverter control output is shown in Fig. 5 and listed in II. As the figure shows, to balance the system, inverters at node 675 and 632 actually *consume* VARs. We believe that this effect occurs as these phase voltages are increasing compared to voltages in the remaining phases.

TABLE II: OPTIMAL INVERTER VAR DISPATCH.

	Phase		
Node	a [pu]	b [pu]	c [pu]
632	-0.0081	-0.0346	0.0437
675	0.005	0.0522	-0.058
680	0.003	0.0011	-0.0038
684	-0.0003	–	-0.0389
Total	-0.0003	0.0187	-0.057

V. CONCLUSION

This paper considered optimization of three phase unbalanced distribution systems. To do so, we derived a linearized model of distribution system power flow that maps real and reactive power injections into squared voltage magnitude differences. This approximate model can be viewed as an extension of the *LinDistFlow* [8] linear model to unbalanced distribution systems. The model itself, although approximate, was also used to give insight into an interesting phenomena regarding voltage rises on lightly loaded phases. As was discussed in the Simulation Results section, a rise in voltage magnitude in one phase can now be attributed to the fact that off diagonal components of (20)-(21) have *opposite* signs of the diagonal components, indicating that large voltage drops in some phases actually contribute to voltage *rises* in others.

Using the linear approximate model, we also developed an Optimal Power Flow (OPF) program to drive system voltages to within a $\pm 5\%$ threshold of 1 p.u. while simultaneously minimizing the squared Euclidian distance between squared voltage magnitudes at each node. Our approach resulted in voltages that were much more balanced at each node, compared to the uncontrolled case.

Although the objective considered in this work was to balance feeder voltages, the derived model is capable of optimizing over a variety of objectives as the equality constraints are now *linear*. Our future work is aimed at exploring other useful applications of three phase unbalanced OPF such as voltage

978-1-5090-4168-8/16/$31.00 ©2016 IEEE

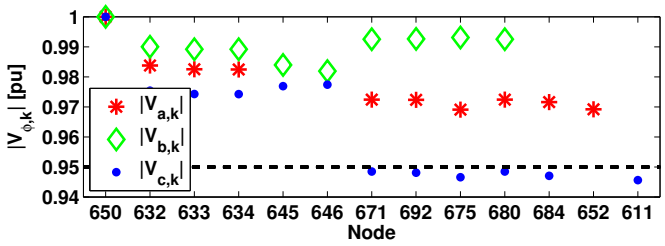

(a) Voltage magnitudes without control.

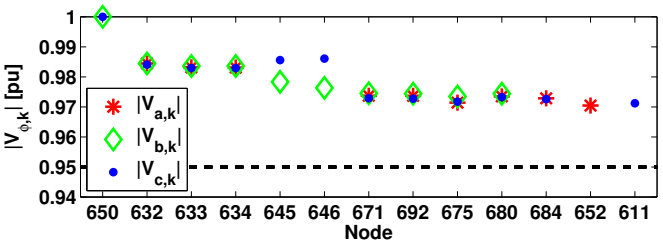

(b) Voltage magnitudes with control.

Fig. 3: Phase a, b, and c voltages magnitudes plotted together for base and control scenarios.

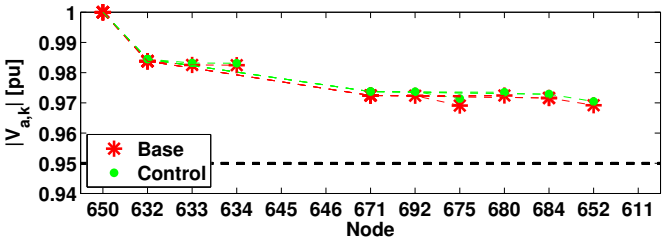

(a) Phase a voltage magnitudes.

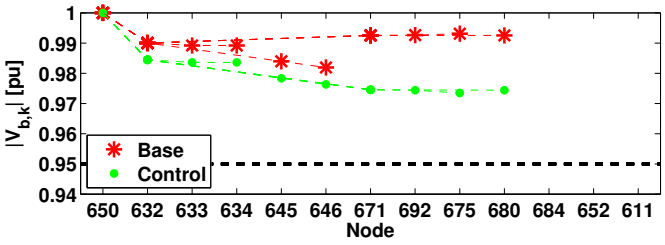

(b) Phase b voltage magnitudes.

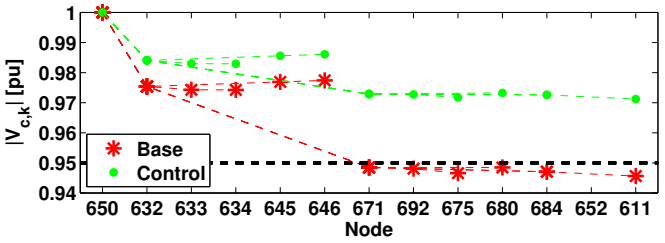

(c) Phase c voltage magnitudes.

Fig. 2: Phase a, b, and c voltages magnitudes for base and control scenarios plotted individually. Dashed lines represent line segments between nodes.

reference tracking, battery and electric vehicle charging, and, perhaps, forecasting.

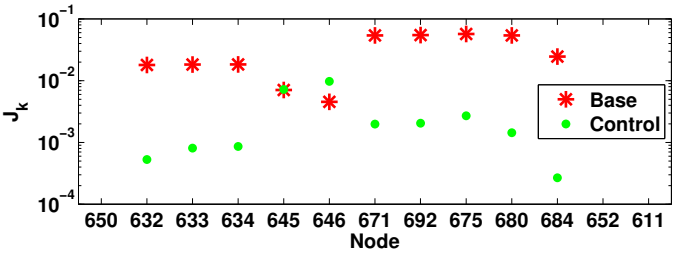

Fig. 4: Phase voltage imbalance for all nodes, as defined in (23).

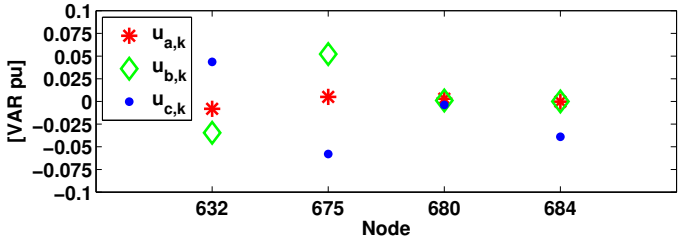

Fig. 5: Optimal inverter VAR resource.

References

[1] E. M. Stewart, S. V. MacPherson, D. Nakafuji, and T. Aukai, "Analysis of high-penetration levels of photovoltaics into the distribution grid on oahu, hawaii, detailed analysis of heco feeder wf1," NREL subcontract report NREL/SR-5500-54494, Tech. Rep.

[2] K. Turitsyn, P. Sulc, S. Backhaus, and M. Chertkov, "Options for control of reactive power by distributed photovoltaic generators," *Proceedings of the IEEE*, vol. 99, no. 6, pp. 1063–1073, 2011.

[3] N. Li, G. Qu, and M. Dahleh, "Real-time decentralized voltage control in distribution networks," in *Communication, Control, and Computing (Allerton), 2014 52nd Annual Allerton Conference on*. IEEE, 2014, pp. 582–588.

[4] B. Robbins, C. N. Hadjicostis, A. D. Domínguez-García *et al.*, "A two-stage distributed architecture for voltage control in power distribution systems," *Power Systems, IEEE Transactions on*, vol. 28, no. 2, pp. 1470–1482, 2013.

[5] B. Zhang, A. D. Dominguez-Garcia, and D. Tse, "A local control approach to voltage regulation in distribution networks," in *North American Power Symposium (NAPS), 2013*. IEEE, 2013, pp. 1–6.

[6] M. Farivar, C. R. Clarke, S. H. Low, and K. M. Chandy, "Inverter var control for distribution systems with renewables," in *IEEE International Conference on Smart Grid Communications (SmartGridComm)*. IEEE, 2011, pp. 457–462.

[7] A. Lam, B. Zhang, A. Dominguez-Garcia, and D. Tse, "Optimal distributed voltage regulation in power distribution networks," *arXiv preprint arXiv:1204.5226*, 2012.

[8] M. E. Baran and F. F. Wu, "Optimal sizing of capacitors placed on a radial distribution system," *IEEE Transactions on Power Delivery*, vol. 4, no. 1, pp. 735–743, 1989.

[9] E. Dall'Anese, G. B. Giannakis, and B. F. Wollenberg, "Optimization of unbalanced power distribution networks via semidefinite relaxation," in *North American Power Symposium (NAPS), 2012*. IEEE, 2012, pp. 1–6.

[10] R. Louca, P. Seiler, and E. Bitar, "Nondegeneracy and inexactness of semidefinite relaxations of optimal power flow," *arXiv*, vol. 1441.4663v1, 2014.

[11] "IEEE Distribution Test Feeders," http://ewh.ieee.org/soc/pes/dsacom/testfeeders/index.html, [Online; accessed May-2015].

978-1-5090-4168-8/16/$31.00 ©2016 IEEE